

The role of porous media in biomedical engineering as related to magnetic resonance imaging and drug delivery

K. Khanafer · K. Vafai

Received: 13 February 2006 / Accepted: 8 May 2006 / Published online: 28 June 2006
© Springer-Verlag 2006

Abstract Pertinent works associated with magnetic resonance imaging (MRI) and drug delivery are reviewed in this work to demonstrate the role of transport theory in porous media in advancing the progress in biomedical applications. Diffusion process is considered significant in many therapies such as delivering drugs to the brain. Progress in development of the diffusion equation using local volume-averaging technique and evaluation of the applications associated with the diffusion equation are analyzed. Tortuosity and porosity have a significant effect on the diffusion transport. Different relevant models of tortuosity are presented and mathematical modeling of drug release from biodegradable delivery systems are analyzed in this investigation. New models for the kinetics of drug release from porous biodegradable polymeric microspheres under bulk erosion and surface erosion of the polymer matrix are presented in this study. Diffusion of the dissolved drug, dissolution of the drug from the solid phase, and erosion of the polymer matrix are found to play a central role in controlling the overall drug release process. This study paves the road for the researchers in the area of MRI and drug delivery to develop comprehensive models based on porous media theory utilizing fewer assumptions as compared to other approaches.

K. Khanafer
Vascular Mechanics Lab, Biomedical Engineering
Department, University of Michigan,
Ann Arbor, MI 48109, USA

K. Vafai (✉)
Mechanical Engineering Department,
University of California, Riverside, CA 92505, USA
e-mail: vafai@enr.ucr.edu

List of symbols

a	Empirical constant
a_E	Einstein radius
ADC	Apparent diffusion coefficient
b	Empirical constant
B_{Sat}	Saturation concentration of the drug in the polymer phase
B_s	Undissolved drug concentration in the polymer
$\langle C \rangle$	Volume average of concentration
C_L	Drug concentration in the liquid phase
C_o	Initial drug concentration
C_{sat}	Saturation concentration of the drug
C_{Se}	Drug concentration in the effective solid phase
C_s	Undissolved drug concentration in the pores
d_p	Pore diameter
D^*	Effective diffusion coefficient
D_B	Polymer diffusion coefficient
ECS	Extracellular space
f_n	Viscosity function
F	Geometric function
F_1, F_2	Correction factors
$F(C)$	Uptake term
h_m	Mass transfer coefficient
k	Permeability
k_{dis}	Dissolution rate constant
k_{ero}	Surface erosion constant
K_B	Forward rate constant
K_C	Backward rate constant
K_{DB}	Dissolution rate constant in polymer
K_{DC}	Dissolution rate constant in pore
K_{Hero}	Hyperbolic erosion rate constant for bulk erosion
K_{Lero}	Linear erosion rate constant for bulk erosion

K_m	Michele-menten constant
K_{Sero}	'S' erosion rate constant for bulk erosion
M_∞	Cumulative amount of drug released at time infinity
M_t	Cumulative amount of drug released at time t
MRI	Magnetic resonance imaging
P	Fluid pressure
r_o	Pore radius
R_s	Radius of microparticles
$\langle s \rangle$	Mass source density
Sh	Sherwood number
t	Time
$\langle v \rangle$	Velocity vector
V	Representative elementary volume
V_1	Effective volume of the microsphere
V_{max}	Rate constant
V_p	Pore volume

Greek symbols

ρ_f	Fluid density
ε	Porosity
λ_g	Geometrical tortuosity
$\lambda_x, \lambda_y, \lambda_z$	Tortuosity components
μ_f	Dynamic viscosity of the pure fluid
σ	Surface area

1 Introduction

Transport phenomena through porous media has been the subject of various studies due to an increasing need for a better understanding of the associated transport processes. This interest stems from numerous practical applications which can be modeled or can be approximated as transport through porous media such as thermal insulation, packed bed heat exchangers, drying technology, catalytic reactors, petroleum industries, geothermal systems and electronic cooling. Vafai and Tien [1, 2] presented an in-depth analysis of the generalized transport through porous media. They developed a set of governing equations utilizing the local volume-averaging technique. The results of this study allowed a simple characterization scheme for interpreting the applicability of Darcy's law for various problems of flow and heat transfer in porous media. In their work the concept of momentum boundary layer and introduction of proper averaging volume for interpreting the results within a momentum boundary

layer were presented. The effects of presence of a solid boundary and inertial forces on the transient mass transfer in porous media were studied by Vafai and Tien [2] with particular emphasis on mass transfer through a porous medium near an impermeable boundary. Some aspects of transport in porous media were discussed in recent monographs by Nield and Bejan [3], Vafai [4, 5], Hadim and Vafai [6] and Vafai and Hadim [7].

Significant advances have been accomplished in applying porous media theory in modeling biomedical applications. Examples include computational biology, tissue replacement production, drug delivery, advanced medical imaging, porous scaffolds for tissue engineering and effective tissue replacement to alleviate organ shortages, and transport in biological tissues [8, 9]. Porous media theory can also be utilized in bio-sensing systems [10–14].

Another important application of porous media includes diffusion process in the extracellular space (ECS) which is crucial for investigating central nervous system physiology. From a physical perspective, the ECS of the brain resembles that of a porous medium. Kuffler and Potter [15] considered the ECS to resemble the water phase of a foam. The ECS constitutes the microenvironment of brain cells and occupies about 20% of nervous tissue volume. It serves as a conduit for cellular metabolites, a channel for chemical signaling mediated by volume transmission, and a route for drug delivery [16]. Therefore, the ECS represents a significant communication channel between neurons, and between neurons and glial cells [17–19]. Recently, Yang and Vafai [8] presented a robust four-layer model to describe low-density lipoprotein (LDL) transport in the arterial wall coupled with the transport in the lumen using porous media theory. Their results are found to be in good agreement with those from the previous experimental and numerical studies under various clinical conditions.

In this work, two applications namely magnetic resonance imaging (MRI) and drug delivery are analyzed as related to the advances in porous media theory in biological applications.

2 Magnetic resonance imaging (MRI)

2.1 Background

Magnetic resonance imaging has become an increasingly important tool in various applications of interest such as clinical diagnostic radiology, porous material

characterization and phase change and dynamics of compounds confined within porous media [20]. In recent years, the bulk of the MRI research work in the literature is focused on clinical applications as related to the detection of acute ischemia, brain diseases such as neurodegenerative and metabolic conditions, infections, and tumors. MRI is a powerful technique for the *in vivo* measurement of the diffusion of water and intracellular metabolites.

Recently, diffusive-weighted magnetic resonance imaging (DW-MRI) has shown superior capabilities compared to other imaging methods because the ischemic brain tissue can be visualized within a very short time period. This technique is primarily due to the water diffusion process. Moreover, DW-MRI technique provides significant information about the structure and the spatial organization of the brain tissue compartments and about the water exchange between these compartments in normal and diseased states [21]. Diffusion process is evaluated in terms of the apparent diffusion coefficient (ADC). The water ADC is considered as an essential parameter in the assessment of stroke patients [22–24].

It has been documented in the literature that several minutes after the onset of the stroke, there is a significant drop in the apparent diffusion coefficient. Because of the clinical importance that diffusion-weighted imaging is likely to have in early detection of stroke; a detailed understanding of the factors that affect ADC of water in tissue is of considerable importance. Norris et al. [25] and Latour et al. [26] concluded that the ADC drop in stroke is due to an increase in the tortuosity of the available pathways for fast diffusion within the extracellular space. Moseley et al. [27], Mintorovitch et al. [28] and Benveniste et al. [29] referred the reduction in the ADC to the cell swelling which causes water molecules to move from extracellular space to the intracellular space, where the diffusion process may be slower, so the overall ADC drops. Helpert et al. [30] have suggested that the reduction in the cell membrane permeability causes a significant decrease in the ADC after acute injury.

2.2 Mathematical modeling of diffusion process using porous media concept

Theoretical models for diffusion process in brain tissues have received less attention by researchers. Greater part of the research related to diffusion process in tissues has been experimentally based. Diffusion in the ECS of the brain, which depends on the ECS porosity and on tortuosity, is quite analogous to

diffusion in porous media composed of two phases (Fig. 1) [31].

Nicholson and Phillips [32] analyzed the diffusion process in the brain-cell microenvironment using the simple diffusion equation in a simple medium with an effective diffusion coefficient and with an altered source term. Mota et al. [33] illustrated that the hindered diffusion model is most suitable for the description of macromolecular diffusion in brain. Dai and Miura [34] built a lattice cellular automate model for ion diffusion within the brain-cell microenvironment and performed numerical simulations using the corresponding lattice Boltzmann equation. The effects of the tortuosity and the volume fraction on the movement of ions by diffusion are analyzed (Fig. 2).

Szafer et al. [35] studied both analytically and numerically water diffusion in a tissue model. The tissue is modeled as a periodic array of boxes surrounded by partially permeable membranes. Expressions for the ADC in isotropic and non-isotropic tissues were derived and compared with Monte Carlo simulations. Nicholson [31] indicated in his report that diffusion is crucial in delivering glucose and oxygen from the vascular system to brain cells as well as in delivering drugs to the brain and in the transport of informational substances between cells, a process known as volume transmission. The structure of brain tissue was represented by the volume fraction (void space) and the tortuosity (hindrance to diffusion imposed by local boundaries or local viscosity). Analysis of these parameters revealed how the local geometry of the brain changes with time under pathological conditions. Nicholson [31] illustrated that the transport of species is significantly affected by an increase in the tortuosity and a decrease in the porosity. For isotropic brain,

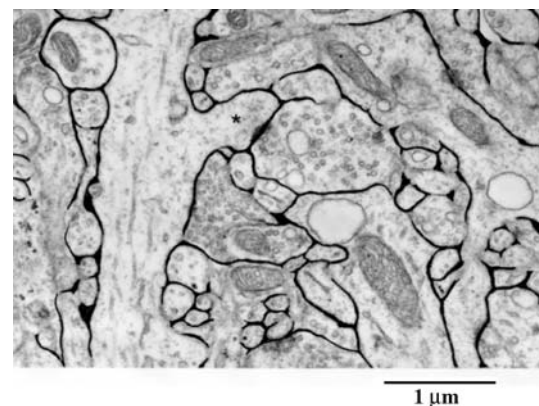


Fig. 1 Electron micrograph of a small region of a rat cerebral cortex with a prominent synapse. The black areas between cells indicate the ECS. (Reprinted from Nicholson [31], with permission from Institute of Physics Publishing)

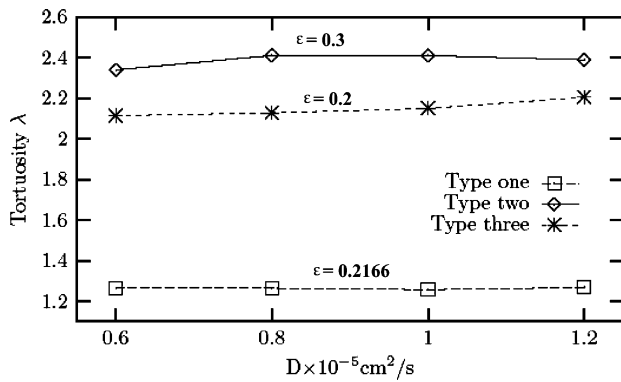


Fig. 2 The effect of diffusion coefficient on the tortuosity for various three-dimensional porous media of different type. (Reprinted from Dai and Miura [34] with permission from SIAM Journal of Applied Mathematics)

Nicholson [31] derived the following diffusion equation:

$$\frac{\partial \langle C \rangle}{\partial t} = D^* \nabla^2 \langle C \rangle + \frac{\langle s \rangle}{\epsilon}, \tag{1}$$

where $\langle C \rangle$, D^* , s , and ϵ are the volume average of the concentration, effective diffusion coefficient of the tissue, mass source density, and volume fraction (porosity), respectively. As mentioned earlier, brain tissue can be treated as a porous medium since it is composed of dispersed cells separated by connective voids to allow for flow of nutrients, minerals, etc. to reach all cells within the brain tissue as depicted in Fig. 1.

Utilizing Fig. 3, the volume average of any arbitrary variable is given by Amiri and Vafai [36], Vafai and Tien [1], Vafai and Tien [2]:

$$\langle \psi \rangle = \frac{1}{V} \int_{V_p} \psi dV \tag{2}$$

with the porosity of the medium expressed as:

$$\epsilon = \frac{V_p}{V}, \tag{3}$$

where V represents a representative elementary volume (REV) of brain tissue, and V_p is the pore volume (ECS) where diffusion takes place. Brain tissues are anisotropic and consequently tortuosity is a second-order tensor. Therefore, the general diffusion equation in Cartesian coordinate can be written as Carslaw and Jaeger [37], Nicholson and Phillips [32]:

$$\frac{\partial \langle c \rangle}{\partial t} = \frac{D}{\lambda_x^2} \frac{\partial^2 \langle c \rangle}{\partial x^2} + \frac{D}{\lambda_y^2} \frac{\partial^2 \langle c \rangle}{\partial y^2} + \frac{D}{\lambda_z^2} \frac{\partial^2 \langle c \rangle}{\partial z^2} + \frac{\langle s \rangle}{\epsilon}, \tag{4}$$

where λ_x , λ_y , and λ_z are the three off-diagonal components of the tortuosity tensor. To describe the

entry and consumption of oxygen by cells, Michaelis-Menten (MM) kinetics are incorporated in the mass diffusion equation [38]. The removal of transmitter substances from ECS such as dopamine (neurotransmitter and hormone) follows this type of kinetics. Therefore, Eq. 1 is changed to the following when MM kinetics exists

$$\frac{\partial \langle C \rangle}{\partial t} = D^* \nabla^2 \langle C \rangle + \frac{\langle s \rangle}{\epsilon} - \frac{V_{\max} \langle C \rangle}{\epsilon(K_m + \langle C \rangle)}, \tag{5}$$

where V_{\max} , which is a function of the type and amount of tissue [39], is a rate constant that represents a measure of the number of uptake sites. Uptake indicates the absorption of some substance, food material, mineral and others by a tissue. The MM K_m constant, which is expressed in units of concentration, is a measure of the dissociation constant for the binding of the substrate (e.g. dopamine) to the membrane uptake sites. To account for uptake or absorption, Lehner [40] proposed the following governing equation for diffusion process using volume averaging procedure:

$$\frac{\partial C}{\partial t} = D^* \nabla^2 C + \frac{s}{\epsilon} - \sigma k(C - C_i), \tag{6}$$

where $\sigma \text{ m}^{-1}$ denotes the surface area of the medium over which the mass transfer process occurs, and k represents a membrane permeability (m/s) (Fig. 3).

2.3 Effective diffusion coefficient and tortuosity

The effective diffusivity is related to the tortuosity of the tissue λ and the diffusivity in the absence of porous medium through the following relations:

$$D^* = \frac{D}{\lambda^2}. \tag{7}$$

For hindered diffusion, $D^* < D$, the effective diffusivity is smaller than the free diffusion coefficient. As such, diffusion is slower in the brain compared to a free medium since the diffusing molecules are slowed down in the convoluted spaces of ECS. The overall tortuosity, λ , is a combination of geometrical and viscous tortuosity as follows [41]:

$$\lambda = \lambda_{\text{geometrical}} \lambda_{\text{viscous}}. \tag{8}$$

El-Kareh et al. [42] introduced an additional viscosity function, f_n , into the definition of the effective diffusivity to take into account the effect of size and nature of diffusing molecules as well as pore wall as shown in Eq. 7:

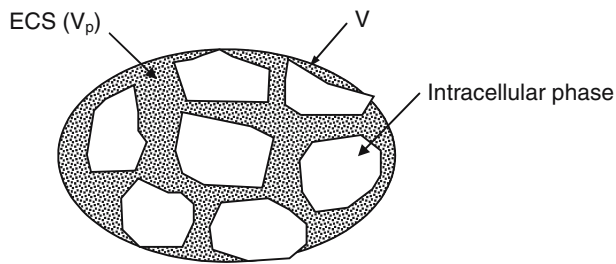


Fig. 3 Schematic diagram for a volume averaging in brain tissue

$$D^* = \frac{D}{(\lambda f_n)^2}. \quad (9)$$

For hindered diffusion, Limbach and Wei [43] and Blanch and Clark [44] expressed the effective diffusivity for diffusion in porous media on a microscopic scale as follows:

$$D^* = D \left(\frac{\varepsilon}{\lambda_g^2} \right) F_1(\gamma) F_2(\gamma); \gamma = \frac{a_E}{r_o}, \quad (10)$$

where a_E is the Einstein radius of the diffusion molecule and r_o is the pore radius, λ_g is the geometrical tortuosity which is a function of porosity and $F_1(\gamma)$ and $F_2(\gamma)$ are correction factors based on the interaction between solute and solvent molecules with the pore. The correction factor $F_1(\gamma)$, which is defined as the ratio of the cross-sectional area of the pore available to the solute molecule divided by the total cross-sectional area of the pore, is defined by:

$$F_1(\gamma) = (1 - \gamma)^2. \quad (11)$$

The correction factor $F_2(\gamma)$ which accounts for the effect of the pore wall on the solvent is given by Deen [45]:

$$F_2(\gamma) = 1 - 2.1044\gamma + 2.089\gamma^3 - 0.948\gamma^5. \quad (12)$$

Netrabukkana et al. [46] expressed the effective diffusivity coefficient for diffusion in a single pore channel ($\varepsilon=1$) assuming a straight cylindrical pore as:

$$D^* = D \times F_1(\gamma) F_2(\gamma). \quad (13)$$

For tortuous pore channel, the effective diffusivity becomes

$$D^* = D \left(\frac{1}{\lambda_g^2} \right) F_1(\gamma) F_2(\gamma). \quad (14)$$

A relationship between porosity and tortuosity was derived by Pfeuffer et al. [47] to describe diffusion of small molecules through ECS in the form of:

$$\lambda = \varepsilon^{-n}. \quad (15)$$

The tortuosity exponent in Eq. 15 depends on the brain tissue behavior. Various studies were conducted in the literature to develop a relationship between tortuosity and porosity using Archie's law [48]. Most of the exponential index values stay between upper and lower border lines covering the vast majority of the experimental points as follows [33]:

$$\text{Upper limit : } n = 0.23 + 0.3\varepsilon + \varepsilon^2 \quad (16)$$

$$\text{Lower limit : } n = 0.23 + \varepsilon^2. \quad (17)$$

Table 1 summarizes various models of the effective diffusion coefficients found in the literature.

Additional studies on the transport of fluids by diffusion inside porous tissues can be seen in the works of Woerly et al. [49] and Koeqler et al. [50]. Woerly et al. [49] analyzed neural tissue formation within porous hydrogels implanted in brain and spinal cord lesions while Koeqler et al. [50] discussed the feasibility of using liquid CO for reducing residual solvents that are used in fabricating biodegradable polymeric devices (Fig. 4).

In the above studies, bulk flow is ignored compared with diffusion process. If bulk flow does occur, then the diffusion equation (5) becomes [31]

$$\frac{\partial \langle C \rangle}{\partial t} + \langle V \rangle \cdot \langle C \rangle = D^* \nabla^2 \langle C \rangle + \frac{\langle s \rangle}{\varepsilon} - F(C), \quad (18)$$

where $\langle V \rangle$ is the bulk flow vector. The uptake term $F(C)$ can be replaced either by

$$\frac{V_{\max} \langle C \rangle}{\varepsilon(K_m + \langle C \rangle)} \quad \text{or} \quad \sigma k(C - C_i). \quad (19)$$

Abbott et al. [51] estimated an average velocity of 10 $\mu\text{m}/\text{min}$ in the cuttlefish assuming porosity of 0.2. Rosenberg et al. [52] and Rosenberg and Kyner [53] predicated a flow velocity of 10.5 $\mu\text{m}/\text{min}$ towards the ventricle in white matter under normal conditions. However, gray matter demonstrated flow only under osmotic stress. Recently, Khaled and Vafai [54] conducted a comprehensive study on the role of porous media on modeling flow and heat transfer in biological tissues. The authors focused on the diffusion process within the brain, diffusion during tissue generation, applications of MRI on categorizing tissue properties, blood flow in tumors, blood flow in perfusive tissues, bioheat transfer in tissues, and bioconvection. Khanfer et al. [55, 56] presented a numerical study on water

Table 1 Various models of effective diffusion coefficient

Reference	Effective diffusion coefficient	Remarks
Present	$D^* = \varepsilon D / \lambda^2$	Hindered diffusion
[98]	$D^* = D / \lambda$	Accounts for porosity Hindered diffusion $\varepsilon = 1$
[31, 32]	$D^* = D / \lambda^2$	Hindered diffusion $\varepsilon = 1$
[70]	$\lambda = \lambda_{\text{geometrical}} \lambda_{\text{viscous}}$ $D^* = D \varepsilon / \lambda$	Hindered diffusion Accounts for porosity
[43, 44]	$D^* = D (\varepsilon / \lambda_g^2) F_1(\gamma) F_2(\gamma)$ $F_1(\gamma) = (1 - \gamma)^2$ $F_2(\gamma) = 1 - 2.1044\gamma + 2.089\gamma^3 - 0.948\gamma^5$	Accounts for porosity Accounts for the interaction between solute and solvent molecules with the pore
[42]	$D^* = D / (\lambda f_n)^2$	$\varepsilon = 1$ Accounts for viscosity
[91]	$D^* = (D / \lambda) \exp[\alpha(\beta - C)]$	$\varepsilon = 1$ Concentration-dependent diffusion coefficient

diffusion within the structure of a brain ECS for various diffusion parameters of brain tissue namely ECS porosity and tortuosity. The ECS was modeled as a homogeneous porous medium with uniform porosity and permeability (Fig. 5).

Concentration maps were developed in this study for various clinical conditions. The effect of the space porosity and the tortuosity on the heat and mass transport within the ECS were found to be significant.

2.4 Generalized momentum equation for fluid flow through a brain tissue

A generalized model is proposed for fluid flow through a brain tissue which accounts for the boundary effects. This can be expressed by

$$\frac{\rho_f}{\varepsilon} \left[\frac{\partial \langle v \rangle}{\partial t} + \langle (v \cdot \nabla) \cdot v \rangle \right] = -\nabla \langle P \rangle^f + \frac{\mu_f}{\varepsilon} \nabla^2 \langle v \rangle - \frac{\mu_f}{K} \langle v \rangle. \quad (20)$$

This equation was obtained through local volume averaging and matched asymptotic expansions [1, 57]. The medium permeability K can be properly modeled [36, 57–59]

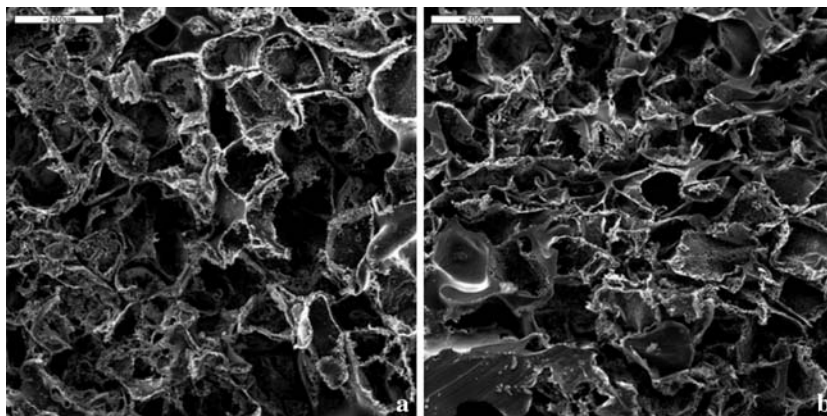
Once the velocity vector is determined, the diffusion equation (18) can be solved for the concentration of substances.

Table 2 illustrates the categorization of diffusion models in brain tissue based on the volume-averaging transport equations for porous medium.

2.5 Proposed generalized diffusion equation

Starting with the diffusion equation for a regular fluid and accounting in the presence of porous matrix and based on the prior diffusion models, the following general diffusion equation is proposed taking into account the variation of porosity and anisotropic properties of the brain tissue

Fig. 4 SEMs of scaffolds after different combinations of salt leaching and CO₂ drying. **a** Salt leached; **b** CO₂ dried, then salt leached. Scale bars are 200 μm . (Reprinted from Koegler et al. [50] with permission from Wiley InterScience)



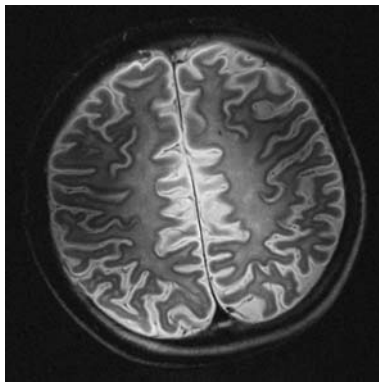


Fig. 5 An axial slice of human cadaver head image acquired just superior to the lateral ventricles using STE-DWI at 8T. The following parameters were used. TR=1,000 ms, TE=75 ms, $\delta=5\text{--}30$ mT/m, $\Delta =40$ ms, FOV=20 cm, slice thickness=2 mm (Reprinted from Khanafer et al. [55] with permission from Elsevier)

$$\frac{\partial \langle C \rangle}{\partial t} + \langle V \rangle \cdot \langle C \rangle = \nabla \cdot [\varepsilon D^* \nabla \langle C \rangle] + \frac{\langle s \rangle}{\varepsilon} - F(C). \quad (21)$$

3 Drug delivery

3.1 Background

Controlled-released drugs delivery to the site of action at a designed rate has numerous advantages over the conventional dosage forms. This interest stems from its importance in reducing dosing frequency, adverse side

effects, and in achieving enhanced pharmacological activity as well as in maintaining constant and prolonged therapeutic effects [60]. The basic formulation of a controlled release of drug consists of an active agent (the drug and excipients) and a carrier which is usually made of polymeric materials [61]. Biodegradable polymers have received considerable attention over the last decade for controlling the drug delivery in the human body without the need to remove the device after treatment. The biodegradable polymers can be used as either matrix devices or reservoirs. In matrix systems, the drug is dispersed or dissolved in the polymer and the release rate of the drug decreases as the time advances. While in reservoir, the drug is encapsulated in a biodegradable membrane. As such the drug is released by diffusion through the membrane at a constant rate. The popularity of this technique has been improved by excellent intrinsic delivery properties of microspheres (membrane). This is due to the small size of microparticles which makes them suitable for direct injection of the drug without requiring surgical implant [62]. Another important feature of the microspheres is that they are made of biodegradable polymers, which degrade and are removed from the human body after the treatment [63].

3.2 Biodegradable drug release systems

The most important mechanisms of controlled release of drugs are diffusion, dissolution, and erosion (bulk and surface). Diffusion mechanism accounts for the

Table 2 Categorization of diffusion models through a brain tissue

Reference	Models	Remarks
Present	$\frac{\partial \langle C \rangle}{\partial t} + \langle V \rangle \cdot \langle C \rangle = \nabla \cdot [\varepsilon D^* \nabla \langle C \rangle] + \frac{\langle s \rangle}{\varepsilon} - F(C)$	Anisotropic Assumes bulk flow Assumes uptake or absorption Accounts for variable Porosity
[31]	$\frac{\partial \langle C \rangle}{\partial t} = D^* \nabla^2 \langle C \rangle + \frac{\langle s \rangle}{\varepsilon}$	Isotropic Neglects bulk flow Neglects uptake or absorption
[31, 32, 37]	$\frac{\partial \langle C \rangle}{\partial t} = \frac{D}{\lambda_x^2} \frac{\partial^2 \langle C \rangle}{\partial x^2} + \frac{D}{\lambda_y^2} \frac{\partial^2 \langle C \rangle}{\partial y^2} + \frac{D}{\lambda_z^2} \frac{\partial^2 \langle C \rangle}{\partial z^2} + \frac{\langle s \rangle}{\varepsilon}$	Anisotropic Neglects bulk flow Neglects uptake or absorption
[31, 40]	$\frac{\partial C}{\partial t} = D^* \nabla^2 C + \frac{s}{\varepsilon} - \sigma k(C - C_i)$	Neglects variable porosity Isotropic Neglects bulk flow Assumes linear uptake process
[31, 38, 39]	$\frac{\partial \langle C \rangle}{\partial t} = D^* \nabla^2 \langle C \rangle + \frac{\langle s \rangle}{\varepsilon} - \frac{V_{\max} \langle C \rangle}{\varepsilon(K_m + \langle C \rangle)}$	Isotropic Neglects bulk flow Assumes non-linear uptake process
[31]	$\frac{\partial \langle C \rangle}{\partial t} + \langle V \rangle \cdot \langle C \rangle = D^* \nabla^2 \langle C \rangle + \frac{\langle s \rangle}{\varepsilon} - F(C)$	Isotropic Assumes bulk flow Assumes uptake or absorption process Neglects variable porosity

diffusion of dissolved drug molecules, while dissolution is a process in which the drug is dissolved from the solid phase. Erosion mechanism stands for the volume loss of the polymer carrier due to the hydrolysis and unraveling of the polymer chains. The coupling among these mechanisms is considered complicated but it is important in describing the release of drug from a biodegradable polymer. Most polymers exhibit bulk erosion where the polymer matrix becomes highly porous due to the penetration of the external fluid as time advances. In the case of surface erosion, polymer degradation occurs mainly in the outmost polymer layers and consequently, erosion affects only the surface and not the inner parts of the polymer as depicted in Fig. 6.

3.3 Mathematical modeling of biodegradable controlled drug systems

Mathematical simulations of drug release from biodegradable micro- and nano-particles, are essential to optimize the design of a therapeutic device. Particles are usually ingested or implanted to deliver the desired amount of drug that may last for a prolonged period of time. Feng and Chien [64] presented a comprehensive analysis of mathematical models to study drug release from nanoparticles.

3.3.1 Diffusion-controlled drug delivery systems

The coupling of diffusion, dissolution, and erosion is complicated but it is important to correctly describe the drug release from a biodegradable carrier. The drug release can be described in the simplest form using Fick's diffusion equation with appropriate boundary conditions [65] and dissolution terms [66] or simplified expressions for erosion-controlled devices [67]. Other models assumed purely erosion or diffusion-controlled cases in regular geometries (slab, cylinder, sphere) using the empirical and semiempirical mathematical models such as Higuchi model [68, 69] and Power law [70–72]. Higuchi model and the power

model were two frequently mathematical models used to describe drug release kinetics. The Higuchi model, valid in devices in which drug concentration is significantly higher than drug solubility, is expressed as

$$\frac{M_t}{A} = [D(2C_o - C_s)C_s t]^{0.5}, \quad (22)$$

where M_t is the cumulative amount of drug released at time t , D is the drug diffusion coefficient, A is the surface area of the controlled release device exposed to the release medium, and C_o and C_s are the initial drug concentration and drug solubility, respectively. The power model which relates the geometry of the system to the drug release mechanism is given by [73]

$$\frac{M_t}{M_\infty} = kt^n, \quad (23)$$

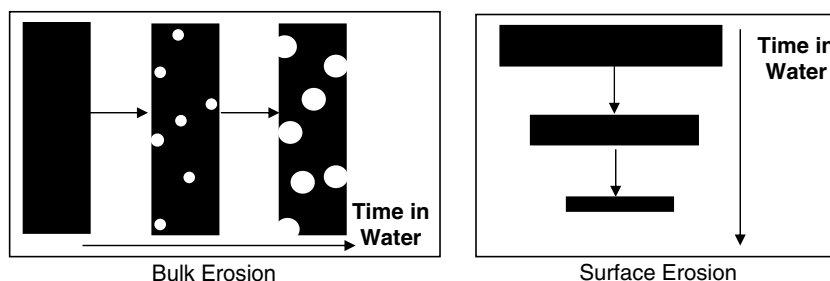
where M_t and M_∞ are the cumulative quantities of drug released at times t and infinity, respectively, and k is a constant associated with the geometry of the device and n is the release exponent. The Weibull function for drug release from a matrix assuming a purely diffusive process and excluding volume interactions between drug molecules is expressed by [74]:

$$\frac{M_t}{M_\infty} = 1 - e^{(-at^b)}, \quad (24)$$

where a and b are empirical constants, respectively.

Siepmann et al. [75] investigated the effect of the composition of diffusion-controlled release devices (type and amount of plasticizer, type of polymer) on the drug diffusivity and the resulting release kinetics in a quantitative way. As previously illustrated in the literature, the rate of drug release mainly depends on the release time, drug diffusivity, drug concentration in the device and the layer thickness of the diffusion barrier [68, 69, 76]. Higuchi [69] modeled the hindering effects of the porous medium by lumping these effects in the definition of the diffusion coefficient ($D^* = D\varepsilon/\lambda$), where ε and λ are the porosity and tortuosity, respec-

Fig. 6 Bulk and surface erosion of a polymer matrix



tively. For a porous matrix biodegradable polymer, erosion mechanism increases the diffusional space by expanding the pore volume and consequently increases the release of drug by diffusion. Siepmann et al. [75] calculated drug release from thin films based on Fick's law of diffusion as follows

$$\frac{M_t}{M_\infty} = 1 - \sum_{n=1}^{\infty} \frac{2\text{Sh}^2}{\beta_n^2 \cdot (\beta_n^2 + \text{Sh}^2 + \text{Sh})} \cdot \exp\left(-\frac{\beta_n^2}{L^2}Dt\right), \quad (25)$$

where M_t and M_∞ are the cumulative amounts of drug release at times t and infinity, respectively, and Sh is the Sherwood number. The β_n values are the positive roots of:

$$\beta \tan \beta = \text{Sh} \quad (26)$$

with

$$\text{Sh} = \frac{h_m L}{D}. \quad (27)$$

The diffusion coefficient of the drug, D , and the mass transfer coefficient, h_m , are determined from experiments (Fig. 7).

The same authors calculated the drug release from microparticles based on Fick's law of diffusion for a sphere assuming infinite mass transfer coefficient in the boundary layer and uniform initial drug concentration as follows:

$$\frac{M_t}{M_\infty} = 1 - \frac{6}{\pi^2} \sum_{n=1}^{\infty} \frac{1}{n^2} \exp\left(-\frac{D \cdot n^2 \cdot \pi^2}{R_s^2}t\right), \quad (28)$$

where R_s is the radius of the microparticles.

3.3.2 Diffusion–erosion controlled drug delivery systems

Many authors in the literature simulated the effect of erosion on diffusion process by allowing the diffusion coefficient to increase with time [77–79]. Hopfenberg [67] derived simplified expressions for erosion-controlled devices assuming that the drug release from erodible slabs, cylinders, and spheres is proportional to the surface area of the device. As such, Hopfenberg [67] derived the following general solution for the cumulative amounts of drug released at time t :

$$\frac{M_t}{M_\infty} = 1 - \left(1 - \frac{k_0 \cdot t}{c_0 \cdot a}\right)^n, \quad (29)$$

where a is the half thickness of a slab or radius of a cylinder or a sphere, c_0 is the initial drug concentration within the drug device, k_0 is the rate constant, M_t and M_∞ are the cumulative amount of drug released at time t and at infinite time, respectively; n is a shape factor ($n=1$ for a slab, $n=2$ for a cylinder, and $n=3$ for a sphere).

Lee [80] proposed a modified version of Higuchi's relations in planar geometry by adding moving erosion front to the dissolution front and assuming that the initial drug loading exceeded the drug solubility in the matrix. Heller and Baker [79] developed a mathematical model describing drug release from thin biodegradable polymer films undergoing bulk erosion and diffusion. They assumed that for polymer matrices undergoing bulk erosion, degradation can be described by first-order kinetics. Joshi and Himmelstein [81] conducted a numerical study on the dynamics of controlled release from bioerodible matrices.

The effects of erosion were simulated by allowing the diffusion coefficient to increase as the concentration of undergraded polymer decreases. A theoretical model was outlined by Batycky et al. [82] for predicting the time evolution of total mass, mean molecular weight, and drug release for the case of a spherical bulk-eroding microsphere, prepared by a double emulsification procedure and containing a hydrophilic drug. Explicit analytical equation was derived for calculating the time evolution of measurable macroscopic characteristics, such as drug release or mean molecular weight. Structural modeling of drug release from biodegradable porous matrices based on a combined diffusion/erosion process was analyzed by Lemaire et al.

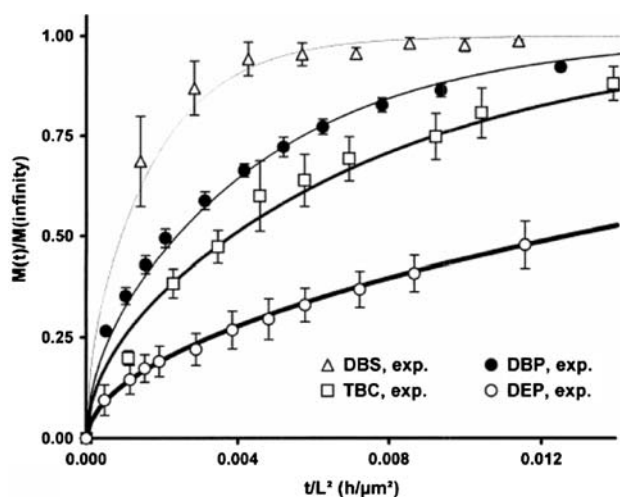


Fig. 7 The influence of the plasticizer type on the drug release rate from thin films (Reprinted from Siepmann et al. [75] with permission from Elsevier)

[83]. The authors gave an expression for the growth of the mean pore radius due to polymer erosion as follows

$$r(t) = r_o + kt, \tag{30}$$

where k is the velocity of erosion and r_o is the initial pore radius. The governing equations were solved numerically in a domain containing a moving surface. The model was confirmed by using release data from biodegradable microspheres with different ratios of low and high molecular weight PLA. The numerical results demonstrated that the relative dominance between diffusion and erosion plays a major role in the release kinetics (Fig. 8).

3.3.3 Diffusion–dissolution controlled drug delivery systems

Lee et al. [84] presented a general model for the release of a drug from porous non-swelling transdermal drug-delivery devices. The processes, which governed the release, were considered to be diffusion of dissolved drug and dissolution of the dispersed drug, both in the body of the device and in the device pores, and transfer of drug between the two domains. The general model is given as follows:

$$\frac{\partial C_L}{\partial t} = D^* \frac{\partial^2 C_L}{\partial z^2} + K_{DC}(\varepsilon C_{Sat} - C_L)f_C(C_s) + K_C B_L - K_B C_L, \tag{31}$$

$$\frac{\partial B_L}{\partial t} = D_B \frac{\partial^2 B_L}{\partial z^2} + K_{DB}[(1 - \varepsilon)B_{Sat} - B_L]f_B(B_s) + K_B C_L - K_C B_L, \tag{32}$$

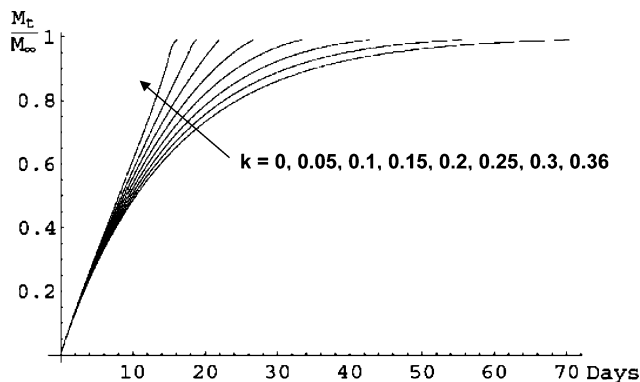


Fig. 8 Temporal variation of the cumulative quantities of drug released drug for various erosion velocity (Reprinted from Lemaire et al. [83] with permission from Elsevier)

$$\frac{\partial C_s}{\partial t} = -K_{DC}(\varepsilon C_{Sat} - C_L)f_C(C_s), \tag{33}$$

$$\frac{\partial B_s}{\partial t} = -K_{DB}[(1 - \varepsilon)B_{Sat} - B_L]f_B(B_s), \tag{34}$$

where C_L is the concentration of the drug dissolved in the pores of the device, B_L is the concentration of the dissolved drug in the polymer, C_s is the undissolved drug concentration in the pores, and B_s is the undissolved drug concentration in the polymer. C_{Sat} and B_{Sat} are the saturation concentration of drug in the solvent and polymer phases, respectively. D^* , which takes into account the effects of pore geometry and topology, is the effective diffusion coefficient in the pore and D_B is the diffusion coefficient in polymer, respectively. K_{DC} and K_{DB} are the dissolution rate constants and $f_C(C_s)$ and $f_B(B_s)$ are functions that determine the changes in the dissolution process as the dispersed phase is depleted. The transfer between the pores and polymer is modeled as a reversible process and the forward (K_B) and backward (K_C) rate constants are related as follows

$$K_C(1 - \varepsilon)B_{Sat} = K_B \varepsilon C_{Sat}. \tag{35}$$

If the drug-delivery device is non-porous and in the classical limits of large dissolution rates, the problem is reduced to one of the moving-boundary type. The solution of this problem in the case where the initial drug loading was much greater than the drug solubility in the device yields expressions for the flux. The pseudo steady-state amount of drug delivered to a perfect sink reduces to the same expression given by as [68, 69]

$$\frac{M_t}{A} = [D(2C_o - C_{Sat})C_{Sat}t]^{0.5}, \tag{36}$$

where $C_o=B_o$, $C_{Sat}=B_{Sat}$, and $D=D_B$.

When $B_{Sat}/B_o \rightarrow 0$, Cohen and Erneux [85] obtained the solution of the unsteady moving-boundary problem as

$$M_t \sim A(2D_B B_{Sat} B_o t)^{0.5}. \tag{37}$$

Harland et al. [66] developed a model of dissolution-controlled, diffusional drug release from porous, non-swellaible polymeric microparticles. Their model incorporated a linear first order dissolution term and transient Fickian diffusion equations and solved for perfect sink and surface dependant boundary conditions. It is assumed that the drug is loaded with an initial concentration of C_o which is higher than the

drug saturation concentration C_{Sat} . The initial system is assumed to have an initial porosity of ε_o . Therefore, the mathematical formulation of the model is expressed as

$$\frac{\partial C}{\partial t} = D^* \left(\frac{\partial^2 C}{\partial r^2} + \frac{2}{r} \frac{\partial C}{\partial r} \right) + k(\varepsilon C_{\text{Sat}} - C)f(C_o - \varepsilon C_{\text{Sat}}), \quad (38)$$

where C is the drug concentration, k is the first order dissolution constant (s^{-1}), ε is the system porosity, and r is the radial position in the sphere. In cases of a concentration-dependent diffusion coefficient, D^* , one may write [86]

$$D^* = \left(\frac{D}{\lambda} \right) \exp[\alpha(\beta - C)] \quad (39)$$

where λ is the tortuosity, and α and β are constants. The dissolution mechanism is described by a generalized function, f , as follows:

$$f(C_o - \varepsilon C_{\text{Sat}}) = \begin{cases} 0; & C_o \leq \varepsilon C_{\text{Sat}} \\ 1; & C_o > \varepsilon C_{\text{Sat}}. \end{cases} \quad (40)$$

3.3.4 Diffusion–erosion–dissolution controlled drug delivery systems

Siepmann and Peppas [87], Siepmann and Gopferich [88], and Siepmann et al. [89] demonstrated that mathematical modeling of drug release from bioerodible delivery systems is more complex than the modeling of diffusion or swelling controlled devices. As such, chemical reactions such as polymer chain cleavage in bioerodible systems should be included in the theoretical models in addition to mass transport phenomena. Siepmann et al. [89] developed a mathematical model describing all phases of drug release from bioerodible microparticles using Monte Carlo simulations. The authors considered three-dimensional geometry of the devices, drug dissolution, diffusion with non-constant diffusivities and moving boundary conditions, polymer degradation/erosion, and time-dependent system porosities.

Zhang et al. [90] presented comprehensive models to account for the kinetics of drug release from porous, biodegradable polymeric microspheres under different erosion mechanisms. They pointed out the three mechanisms namely diffusion, dissolution, and erosion control the overall drug release process. The erosion of the polymer matrix is usually organized

into two categories namely bulk erosion (or homogeneous) and surface erosion (or heterogeneous). Bulk erosion, where the size of microsphere approximately remains constant, takes place as a result of the external fluid penetration into the microsphere. In surface erosion, the erosion occurs at the external boundary of microsphere resulting in a gradual decrease in the size of microspheres. There are three types of bulk erosion pattern that were observed in the experiments [91–94]. These models are Linear erosion model, S Erosion model, and Hyperbolic erosion model. These models are summarized below as follows [90].

3.3.4.1 Linear bulk erosion model For liquid phase Diffusion takes place and drug enters this phase by dissolution and erosion.

$$\frac{\partial C_L}{\partial t} = \frac{1}{r^2} \frac{\partial}{\partial r} \left(D r^2 \frac{\partial C_L}{\partial r} \right) + \frac{C_{\text{Se}} K_{\text{Lero}}}{A : \text{Diffusion}} - \frac{\frac{\partial C_{\text{Se}}}{\partial t} (1 - K_{\text{Lero}} t)}{C : \text{Dissolution}}. \quad (41)$$

For virtual solid phase The drug concentration (C_S) decreases in this phase as a result of erosion and dissolution and is equal to the amount of drug accumulated in the liquid phase.

$$\frac{\partial C_S}{\partial t} = \frac{\partial C_{\text{Se}}}{\partial t} (1 - K_{\text{Lero}} t) - C_{\text{Se}} K_{\text{Lero}} \quad (42)$$

and

$$C_S = \frac{C_{\text{Se}} \cdot V_1}{V_o} = C_{\text{Se}} \frac{\left(V_o^{1/3} - \frac{K_{\text{Hero}} t}{3} \right)^3}{V_o}. \quad (43)$$

For effective solid phase This phase represents the actual changes in the solid phase.

$$\frac{\partial C_{\text{Se}}}{\partial t} = -k_{\text{dis}}(\varepsilon C_{\text{sat}} - C_L), \quad (44)$$

where C_L is the drug concentration in the liquid phase (kg/m^3), C_{Se} is the drug concentration in the effective solid phase (kg/m^3), K_{Lero} is the linear erosion rate constant for bulk erosion (m/day), k_{dis} is the dissolution rate constant (s^{-1}), C_{sat} is the saturation concentration of the drug (kg/m^3), V_o is the initial volume of the microsphere (m^3), V_1 is the effective volume of the microsphere (m^3) in the virtual solid phase, and ε is the porosity.

3.3.4.2 *S bulk erosion model For liquid phase*

$$\frac{\partial C_L}{\partial t} = \frac{\frac{1}{r^2} \frac{\partial}{\partial r} (Dr^2 \frac{\partial C_L}{\partial r})}{A : \text{Diffusion}} + \frac{\frac{C_{Se} K_{Sero} \cdot b \exp(-t K_{Sero})}{[1 + b \exp(-t K_{Sero})]^2}}{B : \text{Erosion}} - \frac{\frac{\partial C_{Se}}{\partial t} \left(1 - \frac{1}{1 + b \cdot \exp(-t \cdot K_{Sero})}\right)}{C : \text{Dissolution}} \tag{45}$$

For virtual solid phase

$$\frac{\partial C_S}{\partial t} = - \frac{C_{Se} \cdot b \cdot K_{Sero} \exp(-t \cdot K_{Sero})}{[1 + b \cdot \exp(-t \cdot K_{Sero})]^2} + \frac{\partial C_{Se}}{\partial t} \times \left(1 - \frac{1}{1 + b \cdot \exp(-t \cdot K_{Sero})}\right) \tag{46}$$

For effective solid phase

$$\frac{\partial C_{Se}}{\partial t} = -k_{dis}(\varepsilon C_{sat} - C_L) \tag{47}$$

where C_S is the drug concentration in the virtual solid phase (kg/m³), b is a constant, and K_{Sero} is the ‘S’ erosion rate constant for bulk erosion (s⁻¹).

3.3.4.3 *Hyperbolic bulk erosion model For liquid phase*

$$\frac{\partial C_L}{\partial t} = \frac{\frac{1}{r^2} \frac{\partial}{\partial r} (Dr^2 \frac{\partial C_L}{\partial r})}{A : \text{Diffusion}} + \frac{\frac{C_{Se} K_{Hero} \left(V_o^{1/3} - \frac{K_{Hero} t}{3}\right)^2}{V_o}}{B : \text{Erosion}} - \frac{\frac{\partial C_{Se}}{\partial t} \frac{1}{V_o} \left(V_o^{1/3} - \frac{K_{Hero} t}{3}\right)^2}{C : \text{Dissolution}} \tag{48}$$

For virtual solid phase

$$\frac{\partial C_S}{\partial t} = - \frac{C_{Se} K_{Hero} \left(V_o^{1/3} - \frac{K_{Hero} t}{3}\right)^2}{V_o} + \frac{\partial C_{Se}}{\partial t} \frac{1}{V_o} \times \left(V_o^{1/3} - \frac{K_{Hero} t}{3}\right)^3 \tag{49}$$

For effective solid phase

$$\frac{\partial C_{Se}}{\partial t} = -k_{dis}(\varepsilon C_{sat} - C_L), \tag{50}$$

where K_{Hero} is the hyperbolic erosion rate constant for bulk erosion (m/day).

3.3.4.4 *Surface erosion* Surface erosion is generally associated with a gradual decrease in the size of a microsphere. As such, erosion takes place at the external boundary of the polymer, although some external fluid may penetrate into the microsphere. To determine the amount of drug released from the sphere, dissolution of the drug from the solid phase, diffusion of dissolved drug, and erosion of the polymer matrix must be taken into account to calculate drug concentration in liquid and solid phases. Drug concentration in liquid phase is mainly determined by diffusion and dissolution processes whenever the following condition is held: $C_\infty \leq C_L \leq \varepsilon C_s$ and $C_s > C_\infty$. Using Fick’s law of diffusion and taking into account drug dissolution from the solid phase to liquid phase, C_L is determined using the following equation [90]:

$$\frac{\partial C_L}{\partial t} = \frac{\frac{1}{r^2} \frac{\partial}{\partial r} (Dr^2 \frac{\partial C_L}{\partial r})}{A : \text{Diffusion}} + \frac{k_{dis}(\varepsilon C_{sat} - C_L)}{B : \text{Dissolution}}, \tag{51}$$

where C_∞ is the drug concentration in the external fluid, C_{sat} is the drug saturation concentration, εC_{sat} is the effective drug saturation concentration in porous region with porosity ε , and D is the effective diffusion coefficient ($D^* = D_o \varepsilon / \lambda$). The sphere is considered shrinking at a constant linear rate. This is supported by experimental observations for drug release from typical surface-eroding polymers [95–97]. Therefore, the radius of the microsphere at any time is given by the following equation:

$$r = R_o(1 - k_{ero}t), \tag{52}$$

where R_o is the initial radius of the microsphere and k_{ero} is the surface erosion constant (s⁻¹) (Fig. 9). The governing equation for the drug concentration in the solid phase is given as follows:

$$\frac{\partial C_s}{\partial t} = - \frac{k_{dis}(\varepsilon C_{sat} - C_L)}{A : \text{Dissolution}} \tag{53}$$

4 **Concluding remarks**

The transport theory in porous media including the effect of tortuosity and porosity on the mass transport equation is significant in describing different biomedical applications. These models are successfully applied

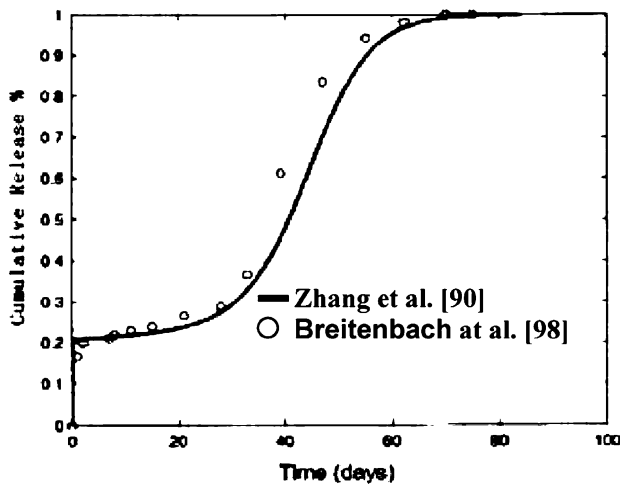


Fig. 9 Temporal variation of the amount of drug released from biodegradable microspheres with bulk erosion models under an infinite mass transfer condition. (Reprinted from Zhang et al. [90] with permission from Wiley InterScience)

in analyzing MRI and drug delivery. They can also be utilized in simulation of blood flow in tumors and muscles. Diffusive transport models are found to play a significant role in the transport of drugs and nutrients to brain cells. Different equations for the effective diffusivity coefficient and tortuosity are summarized and discussed in this work for various conditions. These equations illustrate that tortuosity depends significantly on the porosity of the medium. Mathematical modeling of drug release from biodegradable delivery systems is analyzed in this investigation. New models for the kinetics of drug release from porous biodegradable polymeric microspheres under bulk erosion and surface erosion of the polymer matrix are presented in this study. The mathematical modeling of the mass transfer processes controlling drug release from biodegradable porous matrices is found to substantially depend on the type and size of polymeric microspheres, release time, drug diffusivity, and the composition of drug release. Other effects which count for the drug release system surrounding environment should be included in the structural modeling of drug release systems. These include pH value, cellular tissue reactions, and osmotic pressure.

References

- Vafai K, Tien CL (1981) Boundary and inertia effects on flow and heat transfer in porous media. *Int J Heat Mass Transfer* 24:195–203
- Vafai K, Tien CL (1982) Boundary and inertia effects on convective mass transfer in porous media. *Int J Heat Mass Transfer* 25:1183–1190
- Nield DA, Bejan A (1995) *Convection in porous media*, 2nd edn. Springer, Berlin Heidelberg New York
- Vafai K (2000) *Handbook of porous media*, 1st edn. Marcel Dekker, Inc., New York
- Vafai K (2005) *Handbook of porous media*, 2nd edn. Taylor and Francis Group, New York
- Hadim H, Vafai K (2000) Overview of current computational studies of heat transfer in porous media and their applications-forced convection and multiphase transport. *Adv Numer Heat Transfer* 2:291–330. Taylor and Francis, NY
- Vafai K, Hadim H (2000) Overview of current computational studies of heat transfer in porous media and their applications- natural convection and mixed convection. *Adv Numer Heat Transfer* 2:331–371. Taylor and Francis, NY
- Yang N, Vafai K (2006) Modeling of low-density lipoprotein (LDL) transport in the artery- effects of hypertension. *Int J Heat Mass Transfer* (in press)
- Ai L, Vafai K (2006) A coupling model for macromolecule transport in a stenosed arterial wall. *Int J Heat Mass Transfer* (in press)
- Khaled ARA, Vafai K, Yang M, Zhang X, Ozkan CS (2003) Analysis, control and augmentation of microcantilever deflections in bio-sensing systems. *J Sens Actuators B* 94:103–115
- Yang M, Zhang X, Vafai K, Ozkan C (2003) High sensitivity piezoresistive cantilever design and optimization for analyte-receptor binding. *J Micromech Microeng* 13:864–872
- Khanafar K, Khaled ARA, Vafai K (2004) Spatial optimization of an array of aligned microcantilever biosensors. *J Micromech Microeng* 14:1328–1336
- Khaled ARA, Vafai K (2004) Optimization modeling of analyte adhesion over an inclined microcantilever-based biosensor. *J Micromech Microeng* 14:1220–1229
- Khaled ARA, Vafai K (2004) Analysis of oscillatory flow disturbances and thermal characteristics inside fluidic cells due to fluid leakage and wall slip conditions. *J Biomech* 3:721–729
- Kuffler SW, Potter DD (1964), Glia in the leech central nervous system: physiological properties and neuron-glia relationship. *J Neurophysiol* 27:290–320
- Prokopova-Kubinova S, Vargova L, Tao L, Ulbrich K, Subr V, Sykova E, Nicholson C (2001) Poly [N-hydroxypropyl] methacrylamide] polymers diffuse in brain extracellular space with same tortuosity as small molecules. *Biophys J* 80:542–548
- Nicholson C, Rice ME (1991) Diffusion of ions and transmitters in the brain cell microenvironment. In: Flux K, Agnati LF (eds) *Volume transmission in the brain, novel mechanisms for neural transmission*. Raven Press, New York, pp 279–294
- Nicholson C (1979) Brain cell microenvironment as a communication channel. In: Schmidt FO, Worden FG (eds) *The neurosciences fourth study program*. MIT Press, Cambridge, pp 457–476
- Sykova E (1991) Activity-related ionic and volume changes in neuronal microenvironment. In: Flux K, Agnati LF (eds) *Volume transmission in the brain: novel mechanisms for neural transmission*. Raven Press, New York, pp 217–336
- Barrie PJ (1995) NMR applications to porous solids. *Ann Rep NMR Spectrosc* 30:37–95
- Bose B, Jones SC, Lorig R, Friel HT, Weinstein M, Little JR (1988) Evolving focal cerebral ischemia in cats: spatial correlation of nuclear magnetic resonance imaging, cerebral blood flow, tetrazolium staining, and histopathology. *Stroke* 19:28–37

22. Stejskal EO, Tanner JE (1965) Use of spin-echo pulsed magnetic field gradient to study anisotropic restricted diffusion and flow. *J Chem Phys* 43:3579–3603
23. Taylor DG, Bushell MC (1985) The spatial mapping of translational diffusion by the NMR imaging technique. *Phys Med Biol* 30:345–349
24. Gelderen PV, DeVleeschouwer MH, DesPres D, Pekar J, VanZijl PCM, Moonen CT (1994) Water diffusion and acute stroke. *Magn Reson Med* 31:154–163
25. Norris DG, Niendorf T, Leibfritz D (1993) A theory of diffusion contrast in healthy and infarcted tissue. In: *Proceedings of SMRM, 12th Annual Meeting*. SMRM, New York, 579
26. Latour LL, Svoboda K, Mitra P, Sotak CH (1991) Time dependent diffusion of water in a biological model system. *Proc Natl Acad Sci USA* 91:1229–1233
27. Moseley ME, Cohen Y, Mintorovitch J, Chileuitt L, Shimizu H, Kucharczyk J, Wendland MF, Weinstein PR (1990) Early detection of cerebral ischemia in cats: comparison of diffusion and T₂-weighted MRI and spectroscopy (1990). *Magn Reson Med* 16:330–346
28. Mintorovitch J, Moseley ME, Chileuitt L, Shimizu H, Cohen Y, Weinstein PR (1991) Comparison of diffusion and T₂-weighted MRI for the early detection of cerebral ischemia and reperfusion in rats. *Magn Reson Med* 18:39–50
29. Benveniste H, Hedlund LW, Johnson GA (1992) Mechanism of detection of acute cerebral ischemia in rats by diffusion weighted magnetic resonance microscopy. *Stroke* 23:746–754
30. Helpert JA, Ordidge RJ, Knight RA (1992) The effect of cell membrane water permeability on the apparent diffusion coefficient of water. In: *Proceedings of SMRM, 11th Annual Meeting*, SMRM, Berlin, 1201
31. Nicholson C (2001) Diffusion and related transport mechanisms in brain tissue. *Rep Prog Phys* 64:815–884
32. Nicholson C, Phillips JM (1981) Ion diffusion modified by tortuosity and volume fraction in the extracellular microenvironment of rat cerebellum. *J Physiol* 321:225–257
33. Mota M, Teixeira JA, Keating JB, Yelshin A (2004) Changes in diffusion through the brain extracellular space. *Biotechnol Appl Biochem* 39:223–232
34. Dai L, Miura R (1999) A lattice cellular automated model for ion diffusion in the brain-cell microenvironment and determination of tortuosity and volume fraction. *SIAM J Appl Math* 59:2247–2273
35. Szafer A, Zhong JH, Gore JC (1995) Theoretical model for water diffusion in tissues. *Magn Reson Med* 33:697–712
36. Amiri A, Vafai K (1994) Analysis of dispersion effects and nonthermal equilibrium, non-Darcian, variable porosity incompressible flow through porous media. *Int J Heat Mass Transfer* 37:939–954
37. Carslaw HS, Jaeger JC (1959) *Conduction of heat in solids*, 2nd edn. Clarendon, Oxford
38. Lubarsky DA, Smith LR, Sladen RN, Mault JR, Reed RL (1995) Defining the relationship of oxygen delivery and consumption—Use of biological system models. *J Surg Res* 58:508–803
39. Horn AS (1979) Characteristics of dopamine uptake. In: *Horn AS et al (eds) The neurobiology of dopamine*. Academic, London, pp 217–35
40. Lehner FK (1979) On the validity of Fick's law for transient diffusion through a porous medium. *Chem Eng Sci* 34:821–825
41. Mota M, Teixeira JA, Yelshin A (2001) *Biotechnol Appl Biochem* 17:860–865
42. El-Kerah AW, Braunstein SL, Secomb TW (1993) Effect of cell arrangement and interstitial volume fraction on the diffusivity on monoclonal antibodies in tissue. *Biophys J* 64:1638–1646
43. Limbach KW, Wei J (1990) Restricted diffusion through granular materials. *AIChE J* 36:242–248
44. Blanch HW, Clark DS (1996) *Biochemical engineering*. Marcel Dekker, New York
45. Deen WM (1987) Hindered transport of large molecules in liquid-filled pores. *AIChE J* 33:1409–1425
46. Netrabukkana R, Lourvanij K, Rorrer GL (1996) The Diffusion of glucose and glucitol in microporous and mesoporous silicate catalysts. *Ind Eng Chem Res* 35:458–464
47. Pfeuffer J, Dreher W, Sykova E, Leibfritz D (1998) Water signal attenuation in diffusion-weighted ¹H NMR experiments during cerebral ischemia: influence of intracellular restrictions, extracellular tortuosity, and exchange. *Magn Reson Imaging* 16:1023–1032
48. Archie GE (1942) The electrical resistivity log as an aid in determining some reservoir characteristics. *Trans Am Inst Min Metall Petrol Eng Inc* 146:54–62
49. Woerly S, Petrov P, Sykova E, Roitbak T, Simonova Z, Harvey AR (1999) Neural tissue formation within porous hydrogels implanted in brain and spinal cord lesions: ultrastructural, immunohistochemical, and diffusion studies. *Tissue Eng* 5:467–488
50. Koegler WS, Patrick C, Cima MJ, Griffith LG (2002) Carbon dioxide extraction of residual chloroform from biodegradable polymers. *J Biomed Mater Res Part B* 63:567–576
51. Abbott NJ, Bundgaard M, Cserr HF (1985) Tightness of the blood brain barrier and evidence for brain interstitial fluid flow in the cuttlefish, *Sepia officinalis*. *J Physiol (London)* 368:213–226
52. Rosenberg GA, Kyner WT, Estrada E (1980) Bulk flow of brain interstitial fluid under normal and hyperosmolar conditions. *Am J Physiol* 238:F42–F49
53. Rosenberg GA, Kyner WT (1980) Gray and white matter brain-blood transfer constants by steady-state tissue clearance in cat. *Brain Res* 193:59–66
54. Khaled A-RA, Vafai K (2003) The role of porous media on modeling flow and heat transfer in biological tissues. *Int J Heat Mass Transfer* 46:4989–5003
55. Khanafer K, Vafai K, Kangarlu A (2003) Computational modeling of cerebral diffusion-application to stroke imaging. *Magn Reson Imaging* 21:651–661
56. Khanafer K, Vafai K, Kangarlu K (2003) Water diffusion in biomedical systems as related to magnetic resonance imaging. *Magn Reson Imaging* 21:17–31
57. Vafai K (1984) Convective flow and heat transfer in variable-porosity media. *J Fluid Mech* 147:233–259
58. Vafai K (1986) Analysis of the channeling effect in variable porosity media. *ASME J Energy Resour Technol* 108:131–139
59. Amiri A, Vafai K, Kuzay TM (1995) Effects of boundary conditions on non Darcian heat transfer through porous media and experimental comparisons. *Numer Heat Transfer Part A* 27:651–664
60. Chien YW (1992) *Novel drug delivery systems*, 2nd edn. Marcel Dekker, New York
61. Fan LT, Singh SK (1989) *Controlled release: a quantitative treatment*. Springer, Berlin Heidelberg New York
62. Jalil R, Nixon JR (1990) Biodegradable poly (lactic acid) and poly(lactide-co-glycolide) microcapsules: problems associated with preparative techniques and release properties. *J Microencapsul* 7:297–325

63. Hanes J, Chiba M, Langer R (1998) Degredation of porous poly (anhydride-co-imide) microspheres and implications for controlled macromolecule delivery. *Biomaterials* 19:163–172
64. Feng SS, Chien S (2003) Chemotherapeutic engineering: application and further development of chemical engineering principles for chemotherapy cancer and other diseases. *Chem Eng Sci* 58:4087–4114
65. Crank J (1975) *The mathematics of diffusion*, 2nd edn. Clarendon Press, Oxford UK
66. Harland RS, Dubernet C, Benoit J-P, Peppas NA (1988) A model of dissolution-controlled, diffusion drug release from non-swelling polymeric microspheres. *J Control Release* 7:207–215
67. Hopfenberg HB (1976) Controlled release from erodible slabs, cylinders, and spheres. In: *Controlled release polymeric formulations*. ACS Symposium Series 33:26
68. Higuchi T (1961) Rate of release of medicaments from ointment bases containing drugs in suspension. *J Pharm Sci* 50:874–875
69. Higuchi T (1963) Mechanism of sustained-action medication: theoretical analysis of rate of release of solid drugs dispersed in solid matrices. *J Pharm Sci* 52:1145–1149
70. Peppas NA (1985) Analysis of Fickian and non-Fickian drug release from polymers. *Acta Helv* 60:110–111
71. Kim J, Finn NC (1996) Shape modeling of dissolution profiles by non-integer kinetic orders. *Int J Pharm* 143:223–232
72. Sezer AD, Akbuga J (1995) Controlled release of piroxicam from chitosan beads. *Int J Pharm* 121:113–116
73. Kosmidis K, Argyrakakis P, Macheras P (2003) A reappraisal of drug release laws using Monte Carlo simulations: the relevance of the Weibull function. *Pharm Res* 20(7):988–995
74. Weibull W (1951) A statistical distribution of wide applicability. *J Appl Mech* 18:293–297
75. Siepmann J, Lecomte F, Bodmeier R (1999) Diffusion-controlled drug delivery systems: calculation of the required composition to achieve desired release profiles. *J Control Release* 60:379–389
76. Flynn GL, Yalkowsky SH, Roseman TJ (1974) Mass transport phenomena and models: theoretical concepts. *J Pharm Sci* 63:479–510
77. Charlier A, Leclerc B, Couarraze G (2000) Release of mifepristone from biodegradable matrices: experimental and theoretical evaluations. *Int J Pharm* 200:115–120
78. Bezemer JM, Radersma R, Grijpma DW, Dijkstra PJ, Feijen J, Blitterswijk CA (2000) Zero-order release of lysozyme from poly(ethylene glycol)/poly(butylene terephthalate) matrices. *J Control Release* 64:179–192
79. Heller J, Baker RW (1980) Theory and practice from controlled drug delivery from bioerodible polymers. In: Baker RW (ed) *controlled release of bioactive materials*. Academic Press, New York, pp 1–18
80. Lee PI (1980) Diffusional release of a solute from a polymeric matrix-approximate analytical solutions. *J Membr Sci* 7:255–275
81. Joshi A, Himmelstein KJ (1991) Dynamics of controlled release from bioerodible matrices. *J Control Release* 15:95–104
82. Batycky RP, Hanes J, Langer R, Edwards DA (1997) A theoretical model of erosion and macromolecular drug release from biodegrading microspheres. *J Pharm Sci* 86:1464–1477
83. Lemaire V, Belair J, Hildgen P (2003) Structural modeling of drug release from biodegradable porous matrices based on a combined diffusion/erosion process. *Int J Pharm* 258:95–107
84. Lee AJ, King JR, Hibberd S (1998) Mathematical modeling of the release of drug from porous, nonswelling transdermal drug-delivery devices. *IMA J Math Appl Med Biol* 15:135–163
85. Cohen DS, Erneux T (1988) Free boundary problems in controlled release pharmaceuticals. II: Swelling controlled release. *SIAM J Appl Math* 48:1466–1474
86. Fujita J (1961) Diffusion in polymer-diluent systems. *Fortschr Hochpolym Fortschr* 3:1–47
87. Siepmann J, Peppas N (2001) Modeling of drug release from delivery systems based on hydroxypropyl methylcellulose (HPMC). *Add Drug Deliv Rev* 48:139–157
88. Siepmann J, Gopferich A (2001) Mathematical modeling of bioerodible, polymeric drug delivery systems. *Adv Drug Deliv Rev* 48:229–247
89. Siepmann J, Faisant N, Benoti J-P (2002) A new mathematical model quantifying drug release from bioerodible microparticles using Monte Carlo simulations. *Pharm Res* 19:1885–1893
90. Zhang M, Yang Z, Chow LL, Wang CH (2003) Simulation of drug release from biodegradable polymeric microspheres with bulk and surface erosions. *J Pharm Sci* 92(10):2040–2056
91. James MA, Matthew SS (1997) Biodegradation and biocompatibility of PLA and PLGA microspheres. *Adv Drug Deliv Rev* 28:5–24
92. Breitenbach A, Pistel KF, Kissel T (2000) Biodegradable comb polyesters. Part II. Erosion and release properties of poly(vinyl alcohol)-g-poly-(lactic-co-glycolic acid). *Polymer* 41:4781–4792
93. Wong HM, Wang JJ, Wang CH (2001) In vitro release of human immunoglobulin G from biodegradable microspheres. *Ind Eng Chem Res* 40:933–948
94. Beate B, Christian W, Karsten M, Thomas K (1999) Degradation and protein release properties of microspheres prepared from biodegradable poly-(lactide-co-glycolide) and ABA triblock copolymers: influence of buffer media on polymer erosion and bovine serum albumin release. *J Control Release* 60:297–309
95. Chia HH, Yang YY, Chung TS, Steve NG, Heller J (2001) Auto-catalyzed poly(ortho ester) microspheres: a study of their erosion and drug release mechanism. *J Control Release* 75:11–25
96. Wang JP, Yang YY, Chung TS, Tan D, Steve NG, Heller J (2001) POE-PEG-POE triblock copolymeric microspheres containing protein. II. Polymer erosion and protein release mechanism. *J Control Release* 75:129–141
97. Bear J (1969) Hydrodynamic dispersion. In: de Weist RJM (ed) *Flow through porous media*. Academic Press, New York, pp 109–199
98. Breitenbach A, Pistel KF, Kissel T (2000) Biodegradable comb polyesters. Part II. Erosion and release properties of poly(vinyl alcohol)-g-poly-(lactic-co-glycolic acid). *Polymer* 41:4781–4792